Article

Cell Chemical Biology

Perturbation of Iron Metabolism by Cisplatin through Inhibition of Iron Regulatory Protein 2

Graphical Abstract

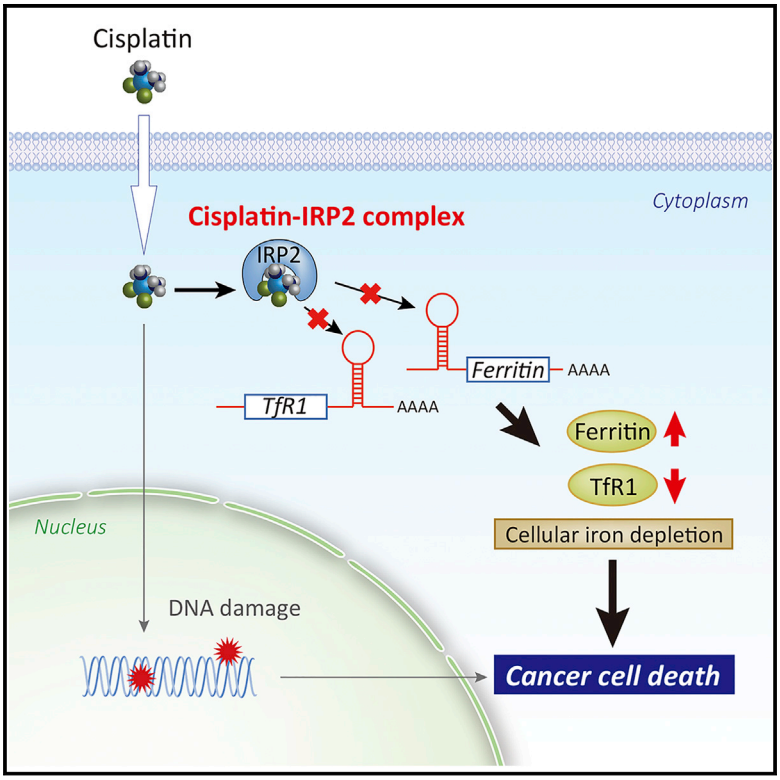

Highlights

- Cisplatin covalently binds to human IRP2 at Cys512 and Cys516
- Cisplatin represses IRP2 binding on ferritin and TfR1 mRNAs (iron metabolism genes)
- IRP2 dysregulation by cisplatin promotes intracellular iron deficiency
- Cisplatin/iron chelator co-treatment potentiates iron deficiency and cancer cell death

Authors

Masaki Miyazawa,
Alexander R. Bogdan, Yoshiaki Tsuji

Correspondence

m.miyazawa@tsc.u-tokai.ac.jp (M.M.),
ytsuji@ncsu.edu (Y.T.)

In Brief

Miyazawa et al. found that the platinum-based anticancer compound cisplatin disrupts the function of iron regulatory protein 2 (IRP2) by adducting to Cys512 and Cys516. Cisplatin-mediated IRP2 inactivation leads to dysregulated iron metabolism and sustained cellular iron deficiency, resulting in cancer cell death *in vitro* and in mouse tumor models.

Miyazawa et al., 2019, Cell Chemical Biology *26*, 85–97
January 17, 2019
https://doi.org/10.1016/j.chembiol.2018.10.009

CellPress

Cell Chemical Biology
Article

Perturbation of Iron Metabolism by Cisplatin through Inhibition of Iron Regulatory Protein 2

Masaki Miyazawa,[1,2,*] Alexander R. Bogdan,[1] and Yoshiaki Tsuji[1,3,*]
[1]Department of Biological Sciences, North Carolina State University, Campus Box 7633, Raleigh, NC 27695, USA
[2]Present address: Undergraduate School of Health Studies, Department of Health Management, Tokai University, Hiratsuka, Kanagawa, Japan
[3]Lead Contact
*Correspondence: m.miyazawa@tsc.u-tokai.ac.jp (M.M.), ytsuji@ncsu.edu (Y.T.)
https://doi.org/10.1016/j.chembiol.2018.10.009

SUMMARY

Cisplatin is classically known to exhibit anticancer activity through DNA damage in the nucleus. Here we found a mechanism by which cisplatin affects iron metabolism, leading to toxicity and cell death. Cisplatin causes intracellular iron deficiency through direct inhibition of the master regulator of iron metabolism, iron regulatory protein 2 (IRP2) with marginal effects on IRP1. Cisplatin, but not carboplatin or transplatin, binds human IRP2 at Cys512 and Cys516 and impairs IRP2 binding to iron-responsive elements of ferritin and transferrin receptor-1 (TfR1) mRNAs. IRP2 inhibition by cisplatin caused ferritin upregulation and TfR1 downregulation leading to sustained intracellular iron deficiency. Cys512/516Ala mutant IRP2 made cells more resistant to cisplatin. Furthermore, combination of cisplatin and the iron chelator desferrioxamine enhanced cytotoxicity through augmented iron depletion in culture and xenograft mouse model. Collectively, cisplatin is an inhibitor of IRP2 that induces intracellular iron deficiency.

INTRODUCTION

Iron is essential for various key enzymes involved in energy metabolism, DNA synthesis, and cell division. Iron deficiency or overload is therefore detrimental to cells and tissues. Iron deficiency impairs iron-dependent enzymes and iron-sulfur clusters and heme-containing proteins, while iron excess increases a risk of production of reactive oxygen species (ROS) through Fenton reaction (Dixon and Stockwell, 2014). Therefore, cellular iron homeostasis has to be tightly regulated by coordinated expression of genes involved in iron transport and storage, such as transferrin receptor-1 (TfR1) and ferritin (Hentze et al., 2010; MacKenzie et al., 2008). These genes are primarily regulated by iron at the post-transcriptional level through interaction between iron regulatory proteins 1 and 2 (IRP1 and IRP2) and iron-responsive element (IRE) located in the 3′ UTR of TfR1 mRNA and 5′ UTR of ferritin mRNA (Anderson et al., 2012; Kuhn, 2015). The binding of IRPs to the IREs is inversely correlated with intracellular iron levels: iron overload disrupts and iron deficiency promotes the binding of IRPs to the IREs (Anderson et al., 2012; Kuhn, 2015). In iron-deficient conditions, the binding of IRPs to 3′ TfR1 IRE increases the stability of TfR1 mRNA, resulting in increased iron transport via TfR1 (Mullner et al., 1989). Concomitantly, the binding of IRPs to the 5′ ferritin IRE results in ferritin translational block, resulting in decreased iron storage into ferritin (Goossen et al., 1990; Muckenthaler et al., 1998). Through this coordinated reciprocal regulation of iron transport and storage by the IRP/IRE regulatory system, cells can also adapt to iron-overload conditions that induce dissociation of IRPs from IREs, resulting in decreased TfR1 mRNA stability and increased ferritin translation (Bogdan et al., 2016; Wang and Pantopoulos, 2011).

Iron is intimately linked with carcinogenesis and tumor progression (Thompson et al., 1991; Toyokuni, 2014). Tumor cells generally require more iron for keeping the active status of proliferation and DNA synthesis (Torti and Torti, 2013). In addition, high iron may cause increased production of ROS that can stimulate growth factor signaling pathways (Ray et al., 2012) along with DNA oxidation and mutations associated with tumor development (Toyokuni, 2014). Indeed, iron overload has been characterized as a risk factor of human carcinogenesis (Selby and Friedman, 1988; Stevens et al., 1988; Toyokuni, 2014). These results suggest the important roles of IRPs (IRP1 and IRP2) in determining cellular iron availability and proliferation capability. Of note, the majority of IRP1 contains stable 4Fe-4S clusters that do not allow IRP1 to bind IREs, instead serves as a cytosolic aconitase in physiologic conditions (Meyron-Holtz et al., 2004). Unlike IRP1, IRP2 has no iron-sulfur cluster and was reported to be the dominant IRE-binding protein (Meyron-Holtz et al., 2004). However, it should be noted that IRP1 plays important roles in systemic iron homeostasis by regulating the expression of hypoxia-inducible factor 2α (Wilkinson and Pantopoulos, 2013), intestinal iron metabolism (Galy et al., 2008), and mouse embryonic development demonstrated by the early lethality of IRP1−/− IRP2−/− embryos (Smith et al., 2006). IRP2 binding to IRE in physiologic condition is correlated with IRP2 expression levels, in which IRP2 protein is subject to degradation by iron-induced accumulation of the E3 ubiquitin ligase FBXL5 (Salahudeen et al., 2009; Vashisht et al., 2009). Consistently, IRP2,

but not IRP1, plays a growth-promoting role in breast cancer cells by elevating intracellular labile iron pool (LIP) (Wang et al., 2014). To deplete iron in cancer cells, evaluation of clinically approved iron chelators, such as desferrioxamine (DFO), a siderophore produced by the *Streptomyces pilosus* (Wilson et al., 2016), as well as newer chelator compounds such as 3-AP, have been underway for potential application of human cancer chemotherapy (Lui et al., 2015; Torti and Torti, 2013).

Platinum-based drugs, such as cisplatin and carboplatin, have been widely used for treatment of solid tumors such as breast, ovarian, testicular, head and neck, and bladder cancers (Dasari and Tchounwou, 2014; Kelland, 2007). General understanding of the anticancer mechanism of these platinum compounds is DNA crosslinking coupled with inhibition of DNA replication and apoptotic cell death after they pass the nuclear membrane (Dasari and Tchounwou, 2014; Kelland, 2007). In addition, some studies demonstrated the direct interaction between cisplatin and proteins (Karasawa et al., 2013; Will et al., 2008); however, it remains largely unknown whether cisplatin-protein interactions play any important biological roles. In this study, we found that cisplatin, but not carboplatin, transplatin, or platinum chloride, binds to human IRP2 at Cys512 and Cys516 in the IRE-binding cleft and impairs IRP2 binding to IREs. Inhibition of IRP2 by cisplatin caused sustained upregulation of ferritin and downregulation of TfR1, resulting in cellular iron deficiency leading to growth inhibition and cell death. Importantly the cisplatin toxicity was ameliorated when iron was supplied or the cisplatin binding sites of IRP2 were mutated. The notable difference between iron chelators and cisplatin, although both cause cellular iron deficiency, is that iron deficiency induced by iron chelation allows cells to stimulate feedback activation of IRP2 and the IRP/IRE system to recover iron levels, whereas cisplatin does not allow cells to do so due to the direct inhibition of IRP2. Furthermore, combination of cisplatin and the iron chelator DFO enhanced anticancer activity in a mouse xenograft model through augmented iron depletion. These insights into the inhibition mechanism of IRP2 by cisplatin and its impact on cell growth should shed light on the IRE/IRP system, particularly IRP2, as a molecular target of xenobiotic toxicity and anticancer approach as well.

RESULTS

Cisplatin Inactivates the IRP/IRE System

During the course of experiments testing whether some chemotherapeutic agents affect expression of iron metabolism genes, we found that cisplatin is a potent inducer of ferritin heavy chain (ferritin H) in SW480 human colon adenocarcinoma cells (Figure 1A) and several other human cell types (Figure S1). This effect was seen in cisplatin treatment but not in carboplatin, transplatin (Figure 1A), or platinum chloride ($PtCl_2$) treatment (Figure S1A). Ferritin H and NQO1 are transcriptionally regulated via the Nrf2-ARE system (Iwasaki et al., 2006); however, we observed no induction of NQO1 protein (Figure 1A) and no increase in ferritin H mRNA levels under cisplatin treatment (Figure 1B), ruling out the involvement of the Nrf2-ARE system. Concomitantly, we observed downregulation of TfR1 protein (Figure 1A) and mRNA (Figure 1B) only by cisplatin treatment. Expression of one isoform of divalent metal transporter 1 mRNA containing a 3′ IRE loop was also suppressed by cisplatin treatment in SW480 cells (Figure S1B).

As both ferritin and TfR1 genes are posttranscriptionally regulated by iron through the IRP/IRE system (Anderson et al., 2012; Kuhn, 2015), we next compared cisplatin with iron during a 24-hr treatment in the expression of ferritin, TfR1, and IRP1 and IRP2. Ferric ammonium citrate (FAC) (100 μM) induced both ferritin H and L proteins and diminished TfR1 protein by 6 hr along with concomitant decrease in IRP2 protein as previously characterized (Salahudeen et al., 2009; Vashisht et al., 2009) (Figure 1C). Cisplatin also induced ferritin H and L by 12 hr, and diminished TfR1 by 24 hr; however, IRP2 protein levels were slightly increased (Figure 1C). The upregulation of ferritin H and downregulation of TfR1 by cisplatin without IRP2 protein degradation was also observed in human HeLa, MCF7, and K562 cells (Figure S1C). Ferroportin, a 5′ IRE loop-containing iron efflux gene primarily expressed in macrophages, hepatocytes, and enterocytes (Drakesmith et al., 2015), demonstrated negligible basal expression that was unaffected by iron or cisplatin treatment in all tested cell lines (Figure S1D); therefore, we consider it unlikely that ferroportin contributes to the observed effects. Furthermore, expression of the 5′ ferritin H IRE-luciferase was induced by cisplatin treatment in SW480 cells (Figure 1D) and HepG2 (Figure S2), and the loss of function by IRE mutation abolished the effect by FAC and cisplatin (Figure 1E), suggesting that cisplatin, like FAC, activates ferritin translation via the 5′ UTR IRE. As IRPs are translational repressors of ferritin 5′ UTR IRE, increased luciferase expression suggests that IRPs and/or the IRP/IRE system was inhibited by cisplatin.

Since cisplatin mimicked most of the iron effects except for downregulation of IRP2 (Figure 1C), we tested whether cisplatin caused iron overload in the cells. We measured intracellular LIP using calcein-AM, a widely adopted fluorescent probe for monitoring iron levels (Ma et al., 2015). The non-fluorescent calcein-AM is converted to a green-fluorescent calcein in cells and its fluorescence is quenched upon binding to intracellular iron. As expected, 100 μM FAC diminished calcein fluorescence in 1.5 hr but returned to untreated levels by 24 hr, indicating that LIP was transiently increased (Figure 1F). In contrast, the calcein fluorescence was significantly enhanced by cisplatin treatment for 12 hr and further for 24 hr (no change at 1.5 hr, not shown), indicating that cisplatin causes sustained LIP depletion rather than iron overload (Figure 1F).

Binding of IRP2 to IRE Is Inhibited in Cisplatin-Treated Cells

Given that the expression of the ferritin 5′ IRE-driven luciferase was increased following cisplatin treatment (Figures 1D and 1E), we tested the possibility of inhibition of the IRP/IRE system as the mechanism of the LIP decrease by cisplatin. First, we tested whether cisplatin inhibits binding of IRPs to the IRE by an RNA-protein pull-down assay. Cell lysates from SW480 treated with cisplatin at 5, 10, and 25 μg/mL for 24 hr were incubated with biotinylated ferritin H IRE RNA, followed by precipitation of the IRE-binding complex with streptavidin-agarose and western blotting with anti-IRP1 and anti-IRP2 antibodies. Cells treated with FAC and the iron chelator DFO were included as controls of decreased and increased IRP/IRE interactions, respectively. Indeed, cisplatin treatment caused decreased

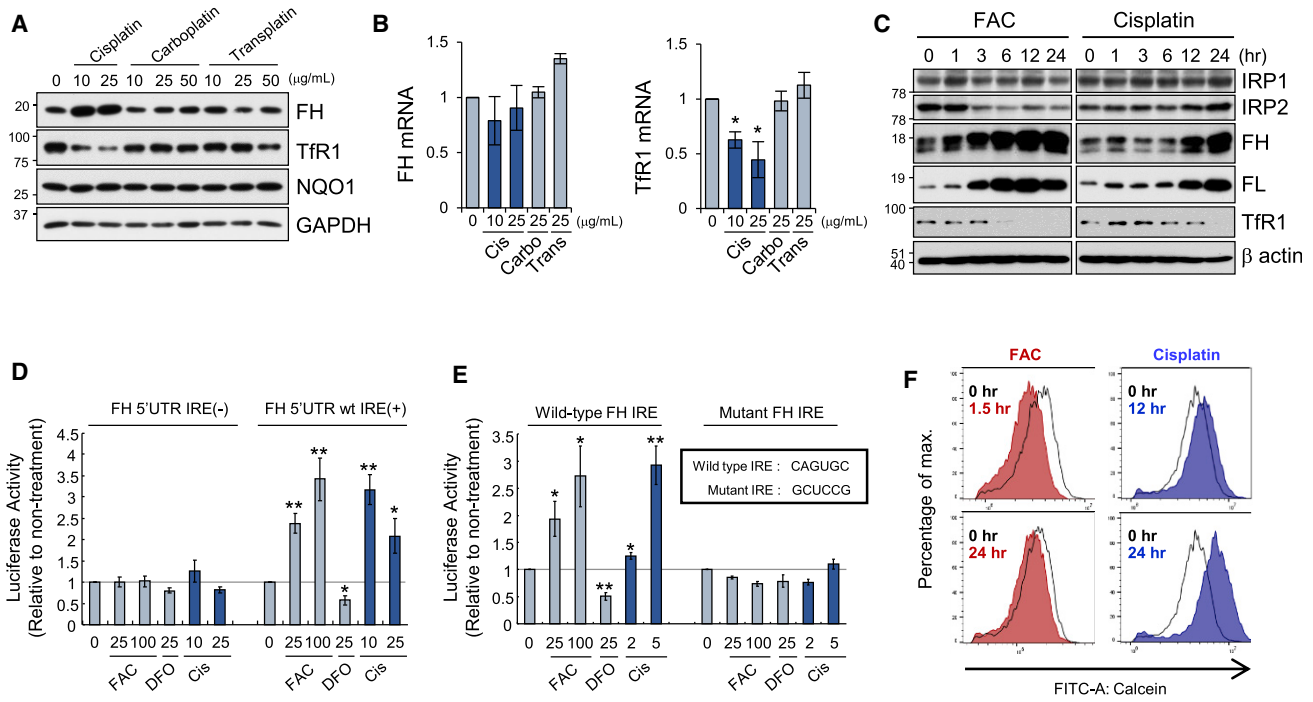

Figure 1. Cisplatin Inactivates the IRP/IRE System

(A and B) Expression of ferritin heavy chain (FH) and transferrin receptor 1 (TfR1) proteins (A) and mRNAs (B) was measured by western blotting and qPCR (normalized with GAPDH mRNA), respectively, in SW480 cells treated with cisplatin, carboplatin, or transplatin for 24 hr. NADPH quinone oxidoreductase 1 (NQO1) and glyceraldehyde 3-phosphate dehydrogenase (GAPDH) proteins were also measured in (A). GAPDH as a protein loading control. Means ± SD are shown (n = 3) in (B). *p < 0.001 versus untreated cells.

(C) Expression of IRP1, IRP2, ferritin H (FH), ferritin L (FL), TfR1, and β-actin (protein loading control) was measured by western blotting in SW480 cells treated with 100 μM ferric ammonium citrate (FAC) or 10 μg/mL cisplatin for 0–24 hr.

(D) Luciferase reporter containing 5′ human ferritin H UTR with or without IRE was transfected into SW480 cells. One day after transfection, cells were treated with 0, 25, or 100 μM FAC, 25 μM DFO, or 10 or 25 μg/mL cisplatin for 12–24 hr, and harvested for luciferase assays. Means ±SD are shown (n = 5–6). *p < 0.05, **p < 0.01 versus untreated cells.

(E) The same luciferase assays as performed in (D) to compare FH wild-type IRE with mutant IRE. Means ±SD are shown (n = 5–6). *p < 0.05, **p < 0.01 versus untreated cells.

(F) Calcein-AM staining was performed in SW480 cells treated with 250 μM FAC for 1.5 and 24 hr (left), 10 μg/mL cisplatin for 12 and 24 hr (right). Representative histograms are shown (n = 4). A 1.5-hr cisplatin treatment showed no shift of the calcein fluorescent peak (not shown).

IRP2 binding to the IRE in a dose-dependent manner, whereas IRP1 binding to the IRE was not inhibited, but rather slightly increased (Figure 2A). To verify this observation in live cells treated with cisplatin, we performed an RNA immunoprecipitation (RIP) assay. Due to poor immunoprecipitation of endogenous IRP1- and IRP2-mRNA complexes with our IRP1 and IRP2 antibodies, we needed transfection of hemagglutinin (HA)-tagged IRP1 or IRP2 into SW480, followed by treatment with cisplatin at 25 μg/mL, immunoprecipitation of HA-IRP/mRNA complex with anti-HA antibody, and RT-PCR to measure co-precipitated ferritin H mRNA. The anti-HA antibody precipitated ferritin H mRNA ten times more efficiently in cells expressing HA-IRP2 than HA-IRP1 (Figure 2B; − cisplatin), suggesting that IRP2 is the major ferritin H IRE-binding protein. Consistent with the pull-down results in Figure 2A, cisplatin treatment slightly increased IRP1 binding but significantly decreased IRP2 binding to the ferritin H mRNA (Figure 2B). In addition, we coincidentally observed that expression of IRP2 in HEK293 cells was undetectable with our anti-IRP2 antibody, in which ferritin expression was unchanged by cisplatin treatment (Figure S3).

These results suggest that the inhibition of IRP2 binding to the IRE by cisplatin caused ferritin upregulation and TfR1 downregulation, as observed in Figure 1. Indeed, endogenous IRP1 knock down had a much weaker effect on endogenous ferritin H, ferritin L, and TfR1 expression compared with IRP2 knockdown showing significant increase in ferritin H and L along with pronounced decrease in TfR1 expression (Figure 2C). IRP1 has been reported to have important roles in systemic iron homeostasis (Galy et al., 2008; Smith et al., 2006; Wilkinson and Pantopoulos, 2013); however, our results suggest that IRP2 is the major regulator of cellular iron homeostasis in our system, consistent with previous studies (Meyron-Holtz et al., 2004; Schalinske et al., 1997). Collectively, these results suggest that cisplatin inhibits IRP2 binding to IRE and the IRP/IRE system.

Cisplatin Directly Inhibits IRP2 for Interaction with IRE

If cisplatin directly inhibits the binding of IRP2 to IRE, there are two targets; IRP2 and the IRE stem loop RNA. First, to test the possibility of direct interaction between cisplatin and IRP2, whole-cell lysates were pre-incubated with cisplatin for 3–24 hr

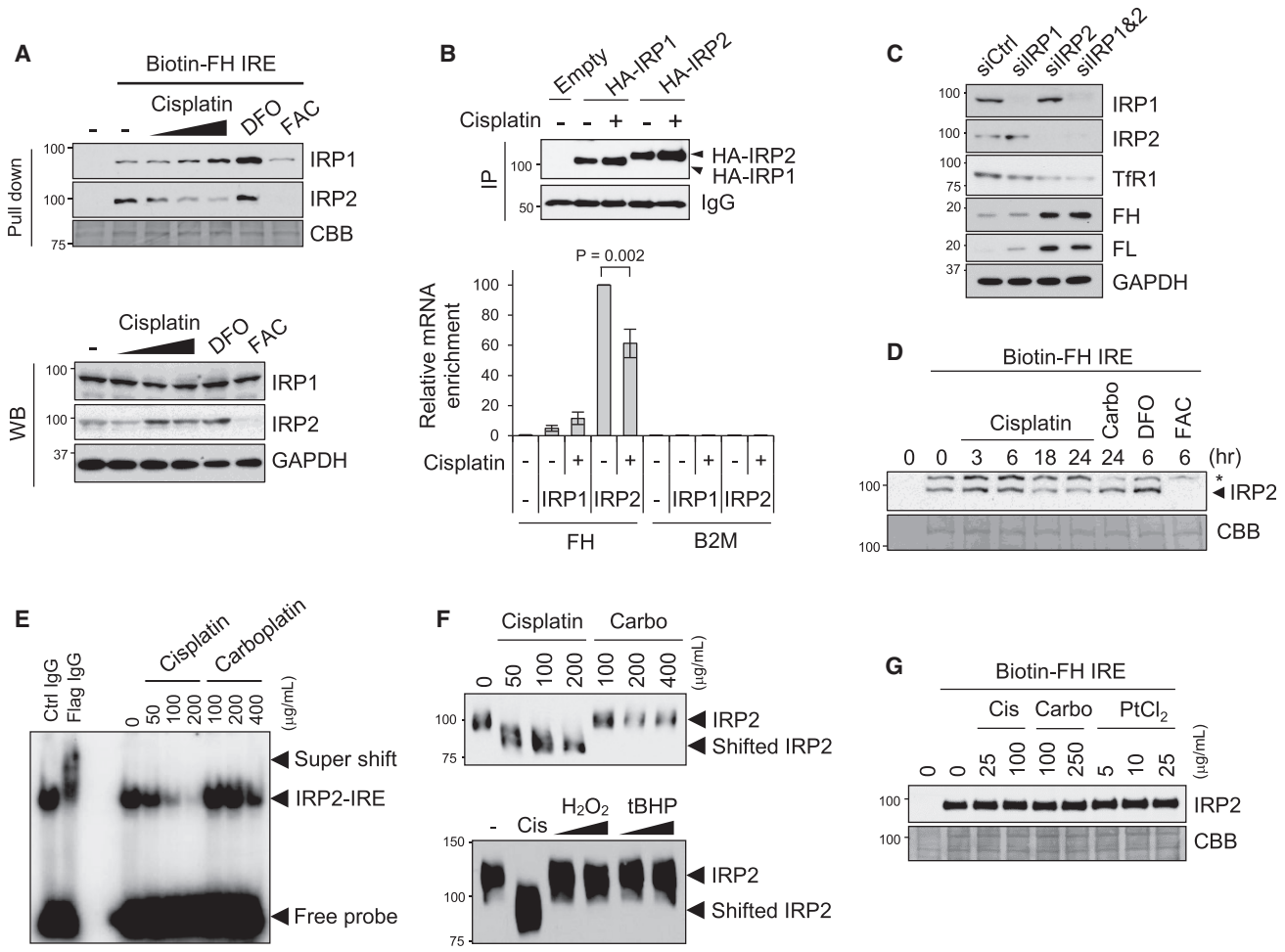

Figure 2. IRP2 Binding to IRE Is Inhibited by Cisplatin

(A) Binding of IRPs to IRE was assessed by pull-down assays using whole-cell lysates from SW480 cells incubated with cisplatin (0, 5, 10, or 25 μg/mL) for 24 hr, DFO (100 μM), or FAC (250 μM) for 10 hr. Whole-cell lysates were incubated with biotinylated ferritin H IRE probe (biotin-FH IRE) and precipitated with streptavidin beads, followed by western blotting with IRP1- and IRP2-specific antibodies. Coomassie brilliant blue (CBB) staining for verification of equal protein loading. IRP1, IRP2, and GAPDH protein levels in the whole-cell lysates were measured by western blotting (WB).

(B) Binding of IRPs to ferritin IRE was assessed by RIP assays. SW480 cells stably transfected with pcDNA3.1/C-HA (empty), HA-IRP1, or HA-IRP2 plasmid were treated with 25 μg/mL cisplatin for 22 hr. Whole-cell lysates were immunoprecipitated (IP) with anti-HA antibody and 10% of IP samples were subjected to western blotting with anti-HA antibody to check IP efficiency (top western blots). Immunoglobulin G (IgG) signal as a loading control. The same IP samples were used for RIP assays for detection of ferritin H (FH) or β_2-microglobulin (B2M) (negative control) mRNA enrichment by qPCR (bottom graph). mRNA enrichment was normalized by input total RNA, and the results are shown as relative mRNA enrichment by IRP2 (– cisplatin, 100%). Means ± SD (n = 3).

(C) siRNA for control (siCtrl), IRP1, or/and IRP2 was transfected into SW480 cells and whole-cell lysates were used for western blots with IRP1, IRP2, TfR1, ferritin H (FH), ferritin L (FL), or GAPDH antibodies.

(D) Whole-cell lysates were incubated with 10 μg/mL cisplatin for 0, 3, 6, 18, or 24 hr, 25 μg/mL carboplatin for 24 hr, 100 μg/mL DFO for 6 hr, or 250 μg/mL FAC for 6 hr in test tubes, and pull-down assay was performed using a biotin-FH IRE probe for detection of IRE-bound IRP2 by western blotting. *Indicates a non-specific band. CBB staining is shown for verification of equal loading.

(E) Human Myc-Flag-tagged IRP2 protein was incubated with cisplatin or carboplatin in the presence of ^{32}P-labeled ferritin H IRE probe. IRP2/IRE complex was separated from the free IRE probe by electrophoresis and visualized by autoradiography. Control IgG or anti-Flag antibody was incubated with samples of Myc-Flag-IRP2 mixed with ^{32}P-IRE probe for verification of the IRP2/IRE interaction as a super shift (left two lanes).

(F) Human Myc-Flag-tagged IRP2 protein was incubated with the indicated concentrations of cisplatin, carboplatin (top), or cisplatin (200 μg/mL), H_2O_2 (0.1 or 1 mM) or tert-butylhydroperoxide (tBHP) (0.1 or 1 mM) (bottom) overnight at room temperature. Samples were loaded on native polyacrylamide gel electrophoresis and subjected to western blotting with anti-IRP2 antibody.

(G) A biotin-FH IRE probe mixed with streptavidin beads was pre-incubated with cisplatin, carboplatin, or $PtCl_2$ overnight. Then, the complex was washed to remove unbound platinum compounds and re-incubated with SW480 whole-cell lysates, and pull-down assay was performed for detection of IRP2/IRE interaction by western blotting. CBB staining for verification of equal protein loading.

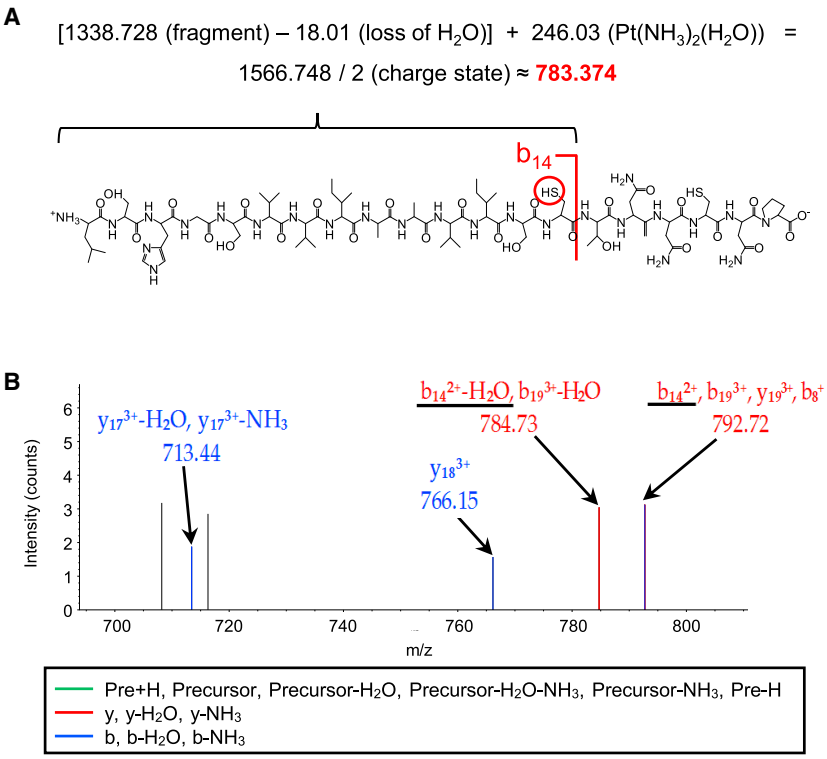

Figure 3. Identification of Cisplatin-IRP2 Adduct Formation by LC/MS/MS

(A) Human Myc-Flag-tagged IRP2 protein was incubated with 500 μg/mL cisplatin for 24 hr at 4°C and liquid chromatography-tandem mass spectrometry (LC-MS/MS) was performed. Platination of Cys512 was manually confirmed by the calculation based on b_{14}-H_2O^{2+} ion of the peptide L^{499}-P^{518} (LSHGSVVIAAVISCTNNCNP).

(B) Zoomed spectrum to Cys512 (b_{14}^{2+}-H_2O and b_{14}^{2+} underlined) is shown.

or carboplatin for 24 hr in test tubes prior to incubation with a biotinylated ferritin IRE RNA probe and pull-down with streptavidin-agarose beads. We observed that the amount of IRP2 precipitated with the IRE probe was decreased at 18 and 24 hr (Figure 2D). To confirm this result, we performed electrophoresis mobility shift assay (EMSA) by pre-incubation of purified Myc-Flag-IRP2 protein with either cisplatin or carboplatin in test tubes, followed by incubation with a radiolabeled ferritin H IRE RNA probe and acrylamide gel electrophoresis. We observed that cisplatin but not carboplatin significantly inhibited IRP2 binding to the IRE probe in a dose-dependent manner (Figure 2E). In addition, we analyzed the EMSA samples of Myc-Flag-IRP2 incubated with cisplatin or carboplatin on native polyacrylamide gel electrophoresis (without 2-mercaptoethanol) and western blotting with anti-Flag antibody. We observed that the IRP2 protein incubated with cisplatin exhibited migration shift (faster migration) than untreated or carboplatin-treated samples (Figure 2F). Furthermore, this migration shift was not likely due to oxidation of IRP2 by cisplatin because incubation of the purified IRP2 with various oxidizing agents, such as 0.1 and 1 mM hydrogen peroxide (H_2O_2) and tert-butyl hydroperoxide did not induce the faster migration (Figure 2F).

Given the propensity of cisplatin to covalently bind to nucleic acid, we also assessed the possibility of the inhibition of the IRP/IRE system through direct binding of cisplatin to the IRE RNA. To this end, we pre-incubated the ferritin H IRE RNA probe with cisplatin, carboplatin, or $PtCl_2$ for 14 hr, and precipitated the IRE probe with streptavidin-agarose to remove unbound platinum compounds. Then, we incubated the pre-incubated ferritin H IRE RNA probe with whole-cell lysates and pulled down the IRE-protein binding complexes with streptavidin-agarose and western blots with anti-IRP2 antibody. As shown in Figure 2G, pre-incubation of cisplatin with the IRE RNA probe did not affect the IRP2 binding, suggesting that direct interaction of cisplatin with the IRE RNA stem loop is not the mechanism of the inhibition of IRP2/IRE interaction. Collectively, these results suggest that cisplatin directly inhibits IRP2 for the binding to the IRE.

Cisplatin Binding at Cys512 and Cys516 of Human IRP2

To identify cisplatin binding sites on IRP2, purified human IRP2 protein incubated with cisplatin was analyzed using liquid chromatography-tandem mass spectrometry. The sequence coverage of the entire IRP2 protein was 98% (Figure S4A). Cisplatin modification sites in the IRP2 protein were searched in peptide fragments mass spectrum, in which the peptide L^{499}~P^{518} (LSHGSVVIAAVISCTNNCNP) was found as a platinated fragment (Figure S4B). Further analyses with Proteome Discoverer 1.4 software (Thermo Scientific) identified the major cisplatin modification site at Cys512 indicated by a mass increase of cisplatin 246.03 [$Pt(NH_3)_2(H_2O)$] on b_{14}-H_2O^{2+} ion (Figures 3A and S4C). We were also able to manually inspect the spectra and confirmed the platination at Cys512 (Figure 3B). In addition to Cys512, we detected the second platination site at Cys516 based on the mass data with a loss of water or ammonia of the b and y ions from the L^{499}~P^{518} peptide (Figures S4D and S4E). Collectively, we concluded that cisplatin directly interacts with the human IRP2 primarily at Cys512 and additionally at Cys516.

Cys512 and Cys516 Mutations Restore IRP2 Function under Cisplatin Treatment

To determine whether cisplatin needs both Cys512 and Cys516 for inhibition of IRP2, we isolated SW480 cells stably transfected with HA-tagged human wild-type (WT) IRP2 and Cys to Ala mutant IRP2 (C512A, C516A, and C512A/C516A) plasmids and tested whether Cys512 and/or Cys516 mutations affects their bindings to IRE and ferritin expression under cisplatin treatment. We also isolated cells stably expressing C578A/C581A IRP2, which is Cys to Ala mutated in the CXXC sequence we found in the human IRP2. This is to test another potential cisplatin adduct site according to the previous report that cisplatin adducts cysteines in the CXXC sequence of the copper chaperon

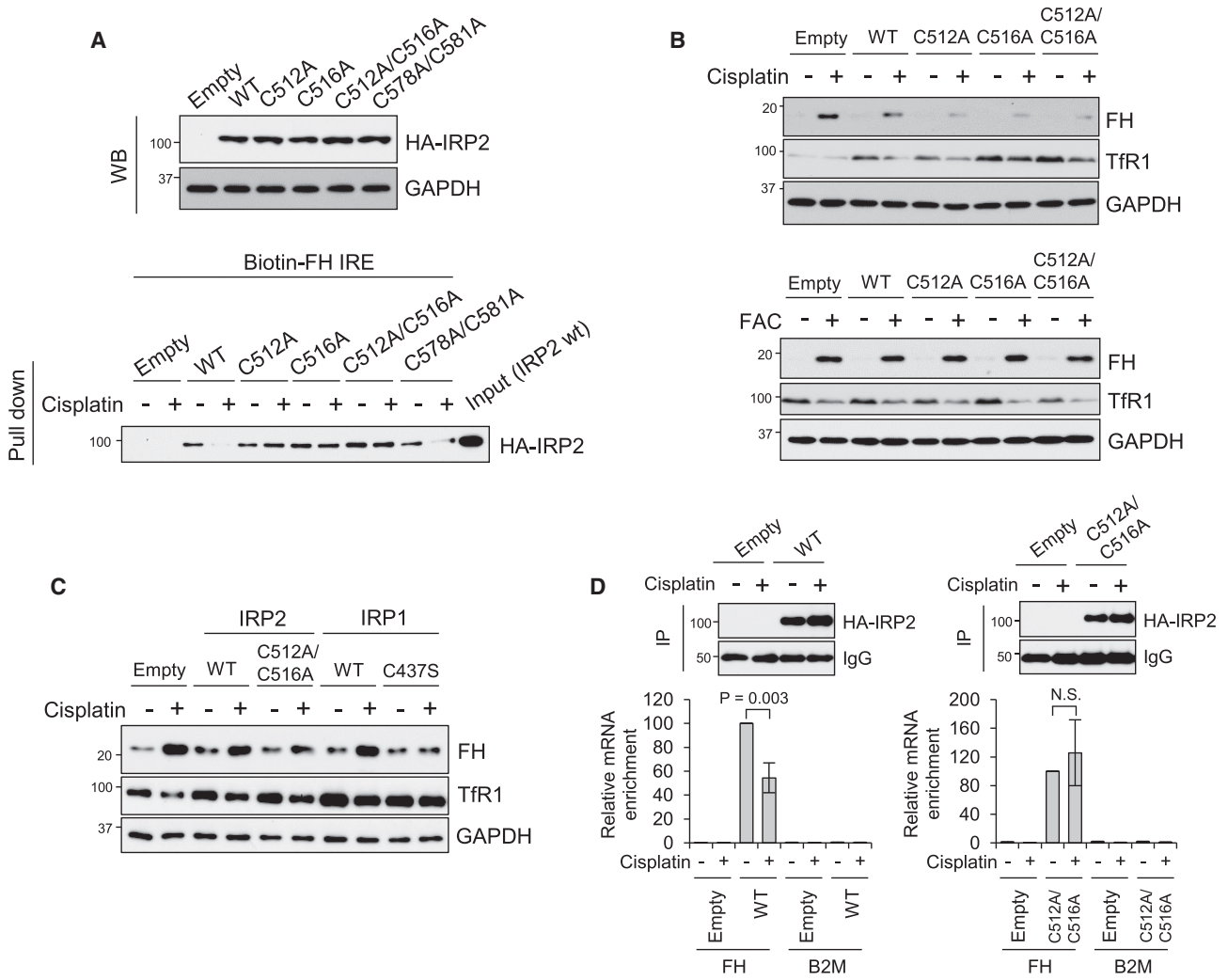

Figure 4. Cys512 and Cys516 Mutations Restore IRP2 Function under Cisplatin Treatment

(A) HA-tagged full-length human IRP2 wild-type (WT) and Cys to Ala mutants (C512A, C516A, C512A/C516A, or C578A/C581A) in pcDNA3.1/C-HA plasmids were stably transfected into SW480 cells. Expression of transfected HA-IRP2 was detected by western blotting with anti-HA antibody, and GAPDH as a loading control (WB, top). These cell lysates were also incubated with 20 μg/mL cisplatin and subjected to pull-down assay using a biotin-FH IRE probe. IRP2 binding to IRE was detected by western blotting with anti-HA antibody (pull-down, bottom).

(B) SW480 cells stably transfected with IRP2 WT and mutants were treated with 10 μg/mL cisplatin for 36 hr (top) or 100 μg/mL FAC for 16 hr (bottom), and western blots were performed with ferritin H (FH), TfR1, and GAPDH antibodies.

(C) SW48 cells stably transfected with empty vector, IRP2 (WT, C512A/C516A) and IRP1 (WT, C437S) were treated with 10 μg/mL cisplatin for 20 hr and western blots were performed with ferritin H (FH), TfR1, and GAPDH antibodies.

(D) pcDNA3 (empty), IRP2WT, or C512A/C516A expressing SW480 cells were treated with 25 μg/mL cisplatin for 22 hr, subjected to RIP assay using anti-HA antibody, followed by qPCR using ferritin H (FH) or B2M primers. Ten percent of IP samples were subjected to western blotting with anti-HA antibody to check IP efficiency (top western blots), and IgG signal as a loading control. RNA enrichment was normalized by input total RNA and results were shown as relative RNA enrichment by WT or C512A/C516A (– cisplatin, 100%). Means ± SD (n = 3) (bottom graphs).

Atox1 protein (Calandrini et al., 2014). They expressed WT and mutant IRP2 proteins equally (Figure 4A, top). Whole-cell lysates were incubated with cisplatin and analyzed for their interactions with the biotin-labeled ferritin IRE probe by pull-down with streptavidin-agarose and western blotting with anti-HA antibody. Without incubation with cisplatin, all IRP2 mutants exhibited equivalent binding to the IRE probe compared with WT IRP2; however, binding of WT IRP2 and C578A/C581A mutant to the IRE probe was significantly diminished when incubated with cisplatin (Figure 4A, bottom). In contrast, C512A, C516A, and C512A/C516A IRP2 were resistant to cisplatin and able to fully bind to the IRE probe (Figure 4A, bottom). These results suggest that the interaction of cisplatin at both Cys512 and Cys516 of IRP2 is necessary to impair the binding of IRP2 to IRE. Similar results were obtained in cell lysates of K562 cells transiently expressing non-tagged IRP2 (Figure S5A).

Instead of incubation of cisplatin and cell lysates in the test tube, we treated these stable WT and mutant IRP2-expressing cells with cisplatin and measured expression of endogenous ferritin H and TfR1 proteins by western blotting. Consistently,

cisplatin treatment highly induced ferritin H expression in pcDNA3 empty vector or WT IRP2-expressing cells, while cells expressing C512A, C516A, and C512A/C516A IRP2 proteins significantly lost the induction of ferritin H synthesis in response to cisplatin treatment (Figure 4B, top). Downregulation of TfR1 by cisplatin was partially rescued in cells expressing these IRP2 mutants (Figure 4B). These results suggest that protection of either Cys512 or Cys516 by Ala substitution makes the IRP2 mutants resistant to inactivation by cisplatin. In other words, inhibition of IRP2 by cisplatin needs both Cys512 and Cys516. Notably, all these WT and mutant IRP2 proteins showed normal response to iron treatment for ferritin upregulation and TfR1 downregulation (Figure 4B, bottom) and normal IRP2 protein stabilization in iron (FAC) or iron chelator (DFO) treatment (Figure S5B). If the inactivation of IRP2 by cisplatin is responsible for ferritin upregulation and TfR1 downregulation, forced expression of an IRP1 mutant that constitutively binds to IREs (C437S) (DeRusso et al., 1995; Wang and Pantopoulos, 2002) should rescue the effects of cisplatin-mediated IRP2 inactivation. To address this question, we treated stably transfected SW480 (empty, WT IRP2, C512A/C516A-IRP2, WT IRP1, and C437S-IRP1) with cisplatin followed by ferritin H and TfR1 western blotting. We found that the IRP1 mutant C437S rescued cisplatin-induced ferritin upregulation and TfR1 downregulation (Figure 4C), suggesting that the IRE-binding form of IRP1 can compensate for cisplatin-induced inactivation of IRP2.

To assess the inhibitory effect of cisplatin on IRP2 through attacking Cys512 and Cys516 in the cells, we performed RIP assays to measure the ferritin IRE and IRP2 interaction in stable WT or C512A/C516A IRP2-expressing cells after treatment with cisplatin. As expected, interaction between the IRE-containing ferritin mRNA and WT IRP2 was significantly diminished by cisplatin treatment, whereas the interaction with C512A/C516A mutant IRP2 was unchanged after cisplatin treatment (Figure 4D). Taken all together, we concluded that cisplatin directly binds to human IRP2 both at Cys512 and Cys516 and inhibits binding of IRP2 to the IREs, resulting in the release of ferritin translation suppression and simultaneous destabilization of TfR1 mRNA as observed in Figures 1A and 1C. The increased ferritin and decreased TfR1 by inhibition of IRP2 can drive more iron storage into ferritin and less iron transport through TfR1 leading to iron deficiency as observed in Figure 1F. This is consistent with the results of IRP2 knockout cells and mouse models (Jeong et al., 2011; LaVaute et al., 2001; Meyron-Holtz et al., 2004; Zumbrennen-Bullough et al., 2014).

Protection of IRP2 Cys512 and Cys516 from the Cisplatin Attack Makes Cells Resistant to Cisplatin Cytotoxicity

Given that IRP2 has growth-promoting and oncogenic functions (Maffettone et al., 2010; Wang et al., 2014), we next tested whether expression of the cisplatin-resistant IRP2 is sufficient for making cells resistant to cisplatin toxicity. To this end, SW480 cells stably expressing HA-tagged IRP2 WT or C512A/C516A equally (Figure 5A) were treated with 20 μg/mL cisplatin for 24 hr and cultured for an additional 48 hr in the normal growth medium, and viable cells were counted. Overexpression of WT IRP2 made cells slightly resistant to cisplatin toxicity (Figure 5B), and C512A/C516A mutant IRP2 made more resistant to cisplatin toxicity, 1.6-fold higher than the pcDNA3 empty vector transfectants (Figure 5B). This was correlated with the weakest activation of caspase-3 by cisplatin treatment in C512A/C516A mutant IRP2-expressing cells (Figure 5C). Cisplatin treatment depleted intracellular iron levels in all three cell types, in which expression of C512A/C516A mutant IRP2 alleviated the iron deficiency more effectively than WT IRP2 (Figure 5D). To further verify the involvement of iron deficiency in cisplatin toxicity, cell viability was measured in cisplatin-treated cells for 1–3 days with or without additional iron in the medium. This assay showed that cisplatin cytotoxicity was alleviated by iron supply (FAC) (Figure 5E). In fact, iron chelator-inducible and pro-apoptotic genes such as GADD45β, p21, and DUSP1 (Saletta et al., 2011; Yu and Richardson, 2011) were remarkably enhanced by cisplatin treatment (Figure 5F). Taken together, iron deficiency induced by cisplatin is involved in its anti-proliferative and apoptotic toxicity mechanisms.

IRP2 Dominates Cancer Cell Survival and Proliferation

Various tumors demand more iron to maintain their rapid cell proliferation and DNA synthesis (Torti and Torti, 2013). TfR1 is overexpressed in many types of cancers (Chan et al., 2014; Habashy et al., 2010; Magro et al., 2011; Prutki et al., 2006). In addition to the transcriptional activation of the TfR1 gene in cancer cells (O'Donnell et al., 2006), TfR1 mRNA can be stabilized by the IRP/IRE system (Miyazawa et al., 2018; Mullner et al., 1989). To validate this possibility in human cancer samples, we searched the relationship between IRPs and TfR1 mRNA expression using RNA sequencing V2 dataset of the breast invasive carcinoma patients (817 samples; Ciriello et al., 2015) in The Cancer Genome Atlas database. In contrast to poor correlation between IRP1 and TfR1 mRNA levels (Pearson's chi-square test, 0.048; Spearman's rank correlation, 0.102), IRP2 expression was well correlated with TfR1 mRNA levels (Pearson's chi-square test, 0.217; Spearman's rank correlation, 0.339) (Figures 6A and 6B). The correlation in the expression levels of TfR1 mRNA and IRP2 better than IRP1 seems to be consistent with the fact that the majority of IRP1 forms a stable iron-sulfur cluster serving as a cytoplasmic aconitase therefore does not participate in binding to IREs in animal tissues (Meyron-Holtz et al., 2004). We also analyzed the relationship between overall survival rates and IRPs mRNA expression in the same breast invasive carcinoma patient data. We found that IRP1 expression levels had marginal correlation with patient's survival rates (Figure 6C), contrasting that a high IRP2 expression group had significantly shorter survival rates than a lower IRP2 expression group (Figure 6D). We also observed that IRP2 contributed to cell survival and proliferation in culture cells. IRP1 knock down or overexpression in SW480 cells showed no effect on TfR1 protein expression and cell viability (Figure 6E). By contrast, IRP2 knock down significantly decreased cell viability versus control (Figure 6F), which was associated with caspase-3 activation compared with siControl (Figure S6). Conversely, IRP2 overexpression increased TfR1 protein and viable cell numbers as well (Figure 6F). These results support the previous reports (Maffettone et al., 2010; Wang et al., 2014) and suggest that IRP2 dominates survival and proliferation of some human cancer cells.

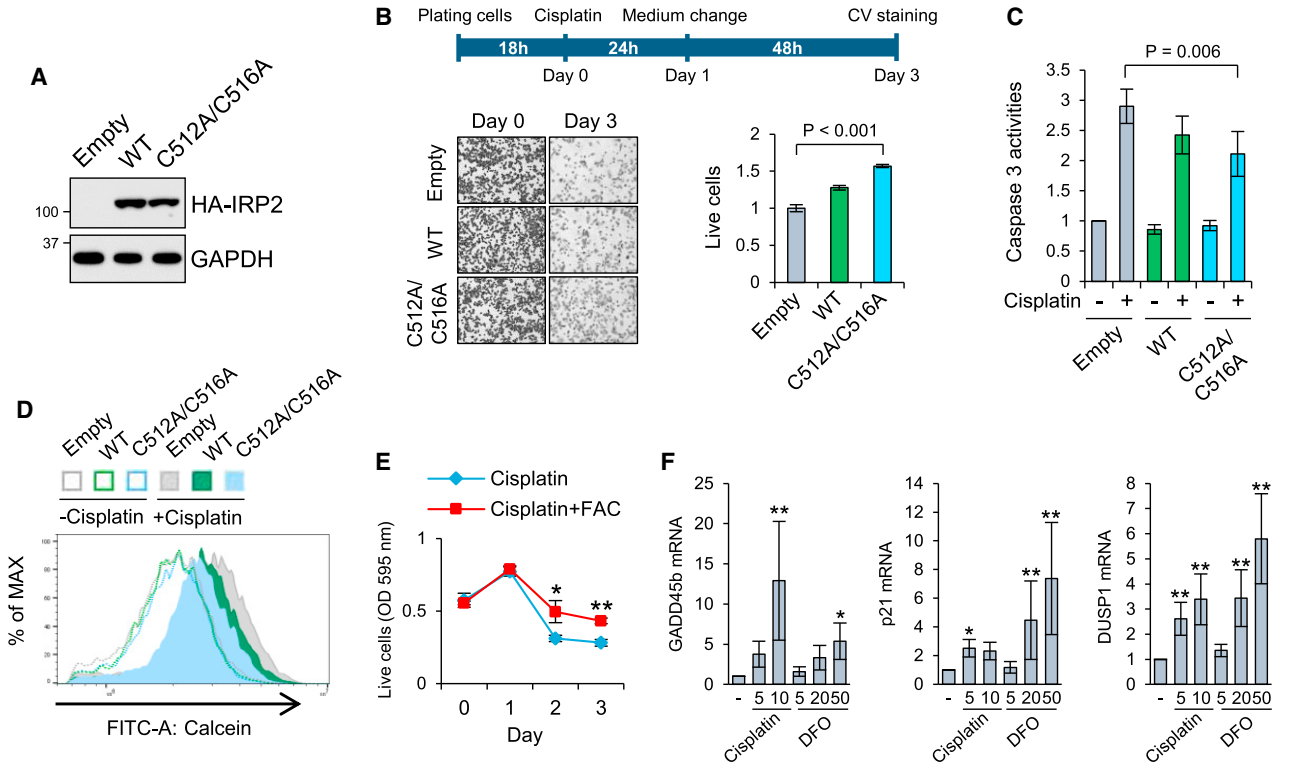

Figure 5. Protection of IRP2 Cys512 and Cys516 from the Cisplatin Attack Makes Cells Resistant to Cisplatin Cytotoxicity

(A) Expression of stably transfected IRP2WT and C512A/C516A IRP2 mutant in SW480 cells were assessed by western blotting with anti-HA antibody.

(B) They were treated with 20 μg/mL cisplatin for 24 hr, and cultured for an additional 48 hr in the normal growth medium. Left panels represent microscopic photographs of cells stained with crystal violet (CV) at day 0 and day 3. CV staining at day 3 was quantitated by normalization with day 0, and the ratio in pcDNA3 transfected cells (empty) was defined as 1. Means ± SD are shown (n = 4).

(C and D) They were treated with 10 μg/mL cisplatin for 16–18 hr and the results of caspase-3 assay in (C) (means ±SD, n = 6) or calcein-AM staining in (D) (a representative histogram from four independent experiments) are shown.

(E) Cell viability was measured by CV staining in SW480 cells treated with 10 μg/mL cisplatin with or without 100 μM FAC for 1–3 days. Means ± SD are shown (n = 3). *p = 0.016, **p < 0.001.

(F) mRNA expression of GADD45β, p21, and DUSP1 was measured by qPCR (normalized by GAPDH or B2M mRNA) in SW480 cells treated with 5 and 10 μg/mL cisplatin, 5, 20, and 50 μM DFO for 20–24 hr, shown as means ± SD (n = 8–16). *p < 0.05, **p < 0.001 versus untreated cells.

Sustained Iron Depletion and Enhanced Cytotoxicity by Combination of Cisplatin and Iron Chelator DFO *In Vitro* and *In Vivo*

Chemotherapeutic strategies using iron chelators for depletion of iron in cancer cells and microenvironment have been elucidated for antineoplastic potential in various human cancers (Lui et al., 2015; Torti and Torti, 2013). Beside the development of several new iron chelators, there were mixed outcomes in regard to their anticancer activities in clinical trials (Lui et al., 2015). The major drawback of iron chelators is that iron deficiency induced by iron chelation is transient by allowing cells to stimulate feedback activation of IRP2 and the IRP/IRE system, resulting in more iron transport and less iron storage to recover from iron deficiency. Given that cisplatin depletes LIP by inactivation of IRP2, we hypothesized that the combination treatment of cisplatin and an iron chelator may decrease LIP more efficiently because the inactivation of IPR2 by cisplatin does not allow cells to reboot the IRP/IRE system. To test this possibility first in cell culture, we measured live cell numbers after treatment with cisplatin, DFO, or cisplatin plus DFO for 5 days. Indeed, cisplatin plus DFO enhanced the cytotoxicity compared with cisplatin or DFO alone, which was ameliorated partially but significantly by adding iron (Figure 7A). Cisplatin and DFO co-treatment further reduced the LIP level compared with cisplatin or DFO alone, which was reverted partially by supplying iron with FAC treatment (Figure 7B).

To evaluate the efficacy of cisplatin and DFO combination in tumor growth *in vivo*, we used a mouse xenograft model by subcutaneous injection of SW480 cells in non-obese diabetic severe combined immunodeficiency gamma immunodeficient mice. After tumor implantation for 10 days, intraperitoneal injection of cisplatin (1 mg/kg) was followed by daily injection of DFO (50 mg/kg) consecutively for 3 days because of short plasma half-life of DFO (Lui et al., 2015). The same administration protocol was repeated four times before harvesting solid tumors (Figure 7C). In this chemotherapy protocol, we observed that cisplatin or DFO alone failed but combination of cisplatin and DFO inhibited the solid tumor growth (Figure 7C). In solid tumors harvested from each treatment group, we found significant ferritin induction and TfR1 downregulation in cisplatin and

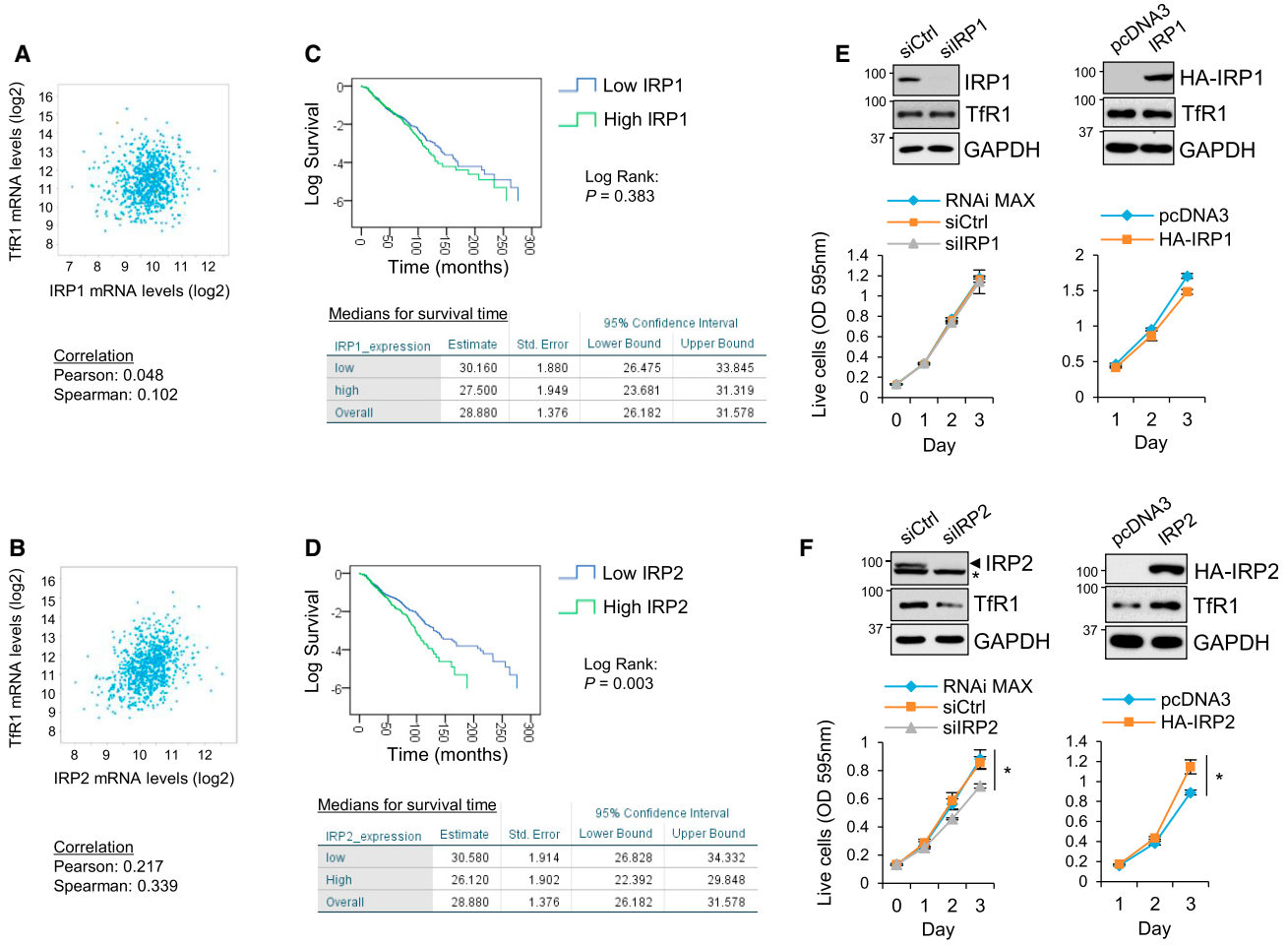

Figure 6. IRP2 Dominates Cancer Cell Survival and Proliferation

(A and B) Scatterplots of expression levels of (A) IRP1, (B) IRP2, and TfR1 mRNAs are shown in breast invasive carcinoma patients (817 samples in The Cancer Genome Atlas database in cBioPortal; Ciriello et al., 2015).

(C and D) Relationship between (C) IRP1, (D) IRP2 mRNA levels and survival rates of the same breast invasive carcinoma patients was calculated by IBM SPSS 24 statistic software. Data from all 817 samples were classified (top 50%, high expression; bottom 50%, low expression group), and Kaplan-Meier estimation and log rank (Mantel-Cox) test were performed between high and low groups (IRP1, p = 0.383; IRP2, p = 0.003).

(E and F) IRP1 (E) or IRP2 (F) siRNA or HA-tagged wild-type IRP1 or IRP2 expression plasmid was transfected into SW480 cells and protein expression levels of IRPs, TfR1, and GAPDH were measured by western blotting (top panels). Cell viability/growth was also measured by crystal violet staining from day 0 to day 3 after transfection and quantitated (bottom graphs). Means ± SD are shown (n = 4–6). *p < 0.001.

cisplatin plus DFO-treated tumors (Figure 7D). Collectively, cisplatin is an inhibitor of IRP2 causing iron depletion and cytotoxicity in a different mechanism from iron chelators and their combination results in an enhanced cytotoxic response due to disruptions in iron metabolism.

DISCUSSION

Cisplatin binds proteins covalently (Karasawa et al., 2013; Will et al., 2008) but little was known about their roles in cisplatin cytotoxicity. In this study we found that cisplatin is an inhibitor of IRP2 through a site-specific interaction that impairs the key regulatory mechanism of cellular iron homeostasis, the IRP/IRE system. Cisplatin causes cytotoxicity through iron deprivation via the IRP2 inhibition, supported by the results that iron supply (Figures 5E and 7A) or expression of cisplatin-resistant mutant IRP2 (Figures 5A–5D) ameliorated the cisplatin cytotoxicity. According to the previous report of cisplatin binding to a Cys-X-X-Cys sequence in the copper chaperone Atox protein (Calandrini et al., 2014), we also tested this sequence as potential cisplatin binding sites in the human IRP2 (Cys578 and Cys581) (Figure 4). These cysteines are conserved in IRP1 at Cys503 and Cys506 located in the region required for IRP1 iron-sulfur cluster formation (Zumbrennen et al., 2009). However, IRP1 was not inactivated by cisplatin (Figure 2A). Furthermore, the C578A/C581A mutant IRP2 behaved similarly to WT IRP2 and lost IRE-binding ability in response to cisplatin treatment (Figure 4A), indicating that these Cys residues are not the cisplatin interaction sites. Instead, our mass spectrometry analyses identified the human IRP2 Cys512 and Cys516 as cisplatin

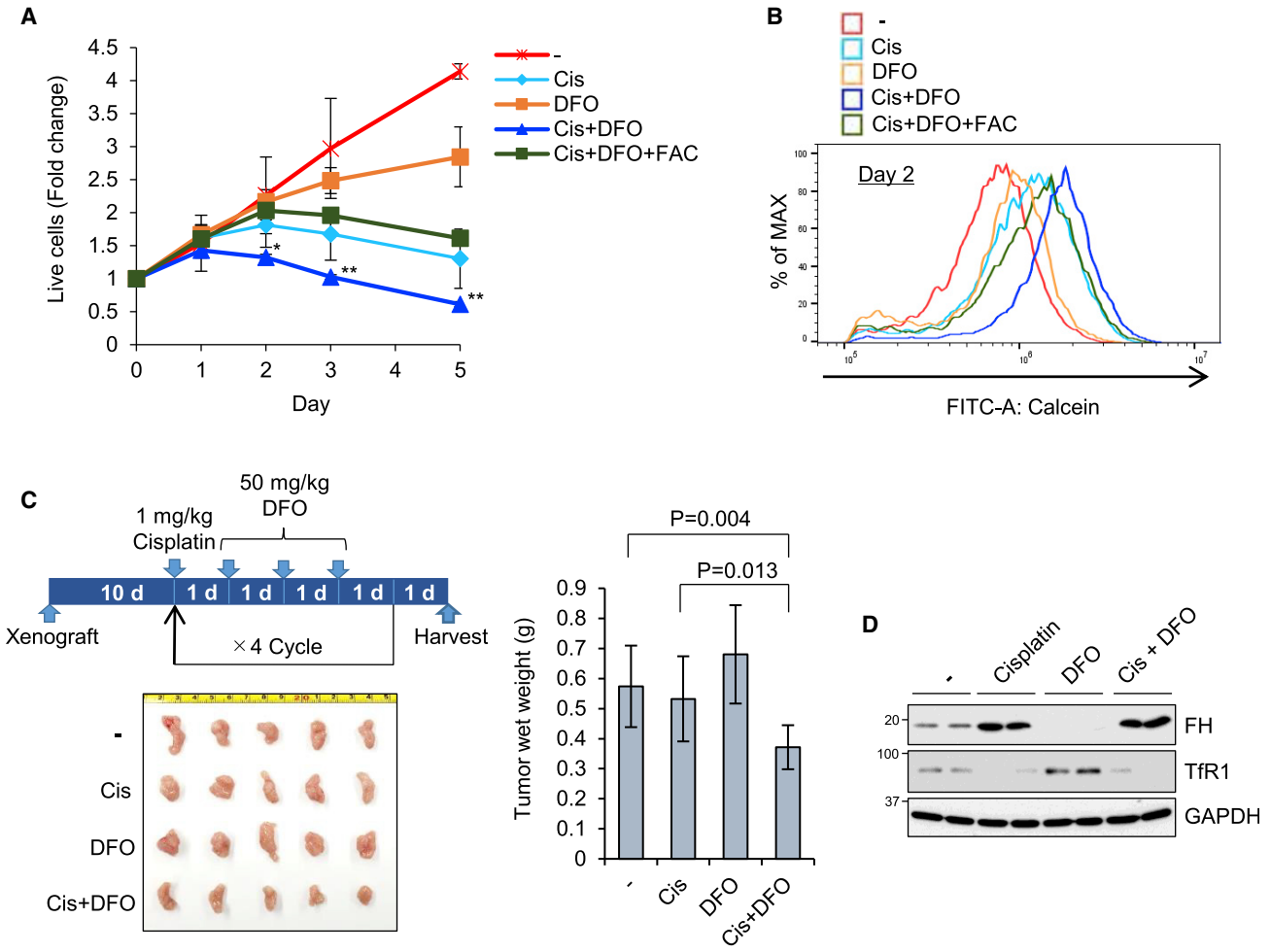

Figure 7. Sustained and Enhanced Iron Deficiency and Toxicity by Combination of Cisplatin and Iron Chelator DFO *In Vitro* and *In Vivo*

(A) SW480 cells were treated with 5 μg/mL cisplatin (Cis), 5 μM DFO, 10 μM FAC, or their combinations for 5 days, and stained with crystal violet. Optical density at 595 nm was measured and normalized with day 0 as 1 in each condition. Means ± SD are shown (n = 3–6). *p < 0.01, **p < 0.001.

(B) The same treatment as (A) for 2 days and calcein-AM staining for LIP were shown (n = 3–6).

(C) SW480 cells were grafted into NSG mice subcutaneously, and 1 mg/kg/day cisplatin and 50 mg/kg/day DFO for 3 days were injected into abdominal cavity. After four cycles of the treatment, these tumors were isolated and wet weight was measured. Means ± SD are shown (n = 6–8).

(D) One day after injection, these tumors were isolated and used for western blotting with ferritin H (FH), TfR1, and GAPDH antibodies.

interaction sites (Figures 3 and S4). These sites are located in the RNA binding cleft of IRP2 (Zumbrennen et al., 2009). It should be noted that these cysteines are able to form a disulfide bond under oxidative stress conditions, which decreased binding of IRP2 to IRE leading to destabilization of TfR1 mRNA (Zumbrennen et al., 2009). In addition, a recent report suggested that Cys512 and Cys516 are potential sites for succination (Kerins et al., 2017). The human IRP2 Cys512 is conserved in IRP1 at Cys437 but IRP2 Cys516 is not conserved, replaced with Ser441 in the human IRP1. Our IRP2/IRE-binding assays demonstrated that cisplatin needed both Cys512 and Cys516 for the inactivation of IRP2 (Figure 4B). Although IRP1 has a minor role in the regulation of the IRP/IRE system in our system (Figure 2C), we anticipate that IRP1 may be resistant to cisplatin for binding to IRE even if Cys437 is modified with cisplatin because of the lack of the second cysteine in IRP1. Notably, mutating IRP1 Cys437 to serine (C437S) creates a form of IRP1 that constitutively binds to IREs and can compensate for IRP2 inactivation by cisplatin (Figure 4C).

No inactivation of IRP2 by carboplatin, transplatin, or platinum chloride (Figures 1A and S1A) may be consistent with the propensity that DNA adduct formation by carboplatin is weaker and slower than cisplatin (Kelland, 2007). Other second-generation platinum compounds such as Nedaplatin, Oxaliplatin, Lobaplatin, and Heptaplatin are structural derivatives of carboplatin having less reactivity and toxicity (Dasari and Tchounwou, 2014; Kelland, 2007). Therefore, like carboplatin, we postulate that these platinum compounds may not cause iron deprivation via the inhibition of IRP2, although it would be necessary to test their effects on IRP2. The lack of IRP2 inhibition may be part of the reason for generally less cytotoxicity and less side effects by these second-generation platinum compounds.

Inhibition of IRP2 by cisplatin caused downregulation of TfR1 and upregulation of ferritin, resulting in significant decrease in

LIP (Figures 1F and 7B). This is consistent with the results in IRP2 knockout mice displaying dysregulation of iron metabolism with iron deficiency due to overexpression of ferritin and downregulation of TfR1 in various tissues including brain (LaVaute et al., 2001), which contributed to the late-onset behavioral impairments or neurodegeneration (Jeong et al., 2011; LaVaute et al., 2001; Zumbrennen-Bullough et al., 2014). Thus, iron deficiency induced by knocking out the IRP2 gene or IRP2 inhibition by cisplatin can cause cytotoxicity. However, the possibility of brain neuronal damage by cisplatin is less likely *in vivo* because cisplatin (and other platinum compounds) poorly crosses the blood-brain barrier (Gregg et al., 1992).

Cancer cells generally require more iron for their aggressive proliferation (Torti and Torti, 2013). This is consistent with the report that increased IRP2 but not IRP1 is responsible for upregulation of TfR1 and downregulation of ferritin in human breast cancer cells, in which IRP2 knock down decreased LIP and inhibited tumor cell growth in a xenograft model (Wang et al., 2014). Thus, higher expression of IRP2 increases LIP and promotes cell proliferation, and vice versa. Furthermore, increased expression of IRP2 was correlated with high-grade human breast cancer (Figure 6D) (Wang et al., 2014). Conversely, another study showed that forced expression of IRP2 promoted growth of lung cancer cells in a xenograft model (Maffettone et al., 2010). These results support the idea that IRP2 is a promising anticancer target. Limiting iron availability using iron chelators is another reasonable antineoplastic approach, in particular using those clinically approved for iron-overload diseases (Lui et al., 2015; Torti and Torti, 2013). However, thus far, no iron chelator has been approved for tumor chemotherapy because of inconclusive outcomes of their effects in clinical trials. The major drawback of iron chelators is that iron deficiency induced by iron chelation allows feedback activation of the IRP/IRE system to transport more iron and adjust the imbalance of iron homeostasis accordingly. By contrast, cisplatin inhibits IRP2 and the IRP/IRE system, but does not allow cells to recover from the iron deficiency (Figure 1F). As shown in Figure 7, combination of lower doses of cisplatin and DFO depletes more intracellular iron than each agent alone. This can be explained by the mechanism that cisplatin inhibits the IRP/IRE system and blocks cellular adjustment of the iron deficiency caused by DFO, which can ultimately enhance the anticancer efficacy of each agent. This study sheds light on the IRP/IRE system, particularly IRP2, as a cellular target for cisplatin and probably some other endobiotics, xenobiotics, and their metabolites.

SIGNIFICANCE

Traditionally, cisplatin anticancer activity was understood to be a function of cisplatin-DNA adduct formation in the nucleus. In addition to this, many proteins bind to cisplatin at specific amino acid sites, but the biological significance of these cisplatin-protein adducts remains poorly defined. Here, we have characterized the effect of a cisplatin-protein adduct associated with cellular iron homeostasis using an *in vitro* culture system as well as mouse xenograft models. We demonstrate that cisplatin directly inhibits the master regulator of iron metabolism, the cytoplasmic protein iron regulatory protein 2 (IRP2), through covalent binding on IRP2 Cys512 and Cys516, which induces intracellular iron deficiency. The cisplatin-induced, IRP2-inactivation-mediated intracellular iron deficiency emerged as a major mechanism of cytotoxicity after cisplatin treatment. These findings help expand our understanding of cisplatin anticancer and side effects due to protein adduct formation and iron metabolism dysregulation in the cytoplasm.

STAR★METHODS

Detailed methods are provided in the online version of this paper and include the following:

- KEY RESOURCES TABLE
- CONTACT FOR REAGENT AND RESOURCE SHARING
- EXPERIMENTAL MODEL AND SUBJECT DETAILS
  - Animal Studies
- METHOD DETAILS
  - Cell Culture and Chemicals
  - Western Blot and Antibodies
  - Real Time PCR
  - Luciferase Assay
  - Pull-Down mRNA-Protein Binding Assay
  - Electrophoresis Mobility Shift Assay (EMSA)
  - Expression Plasmids of IRP1 and IRP2 Mutants
  - Crystal Violet Staining
  - siRNA Transfection
  - Intracellular Free Iron Measurement
  - Caspase 3 Activity Assay
  - RNA Immunoprecipitation (RIP) Assay
  - Identification of Cisplatin-IRP2 Adduct Sites
  - Mice Xenograft
- QUANTIFICATION AND STATISTICAL ANALYSIS

SUPPLEMENTAL INFORMATION

Supplemental Information includes six figures and three tables and can be found with this article online at https://doi.org/10.1016/j.chembiol.2018.10.009.

ACKNOWLEDGMENTS

We are grateful to Dr. Michael Bereman for their initial mass spectrometry analyses and helpful discussion to characterize cisplatin and IRP2 interaction. We thank Drs. Susan Sumner and James Harrington at RTI International for ICP-MS analyses to measure platinum for preliminary characterization of direct interaction between cisplatin and IRP2. We also thank Dr. Jun Ninomiya-Tsuji for helping with our xenograft mouse experiments. This work was supported by NIH grants R01GM088392 and R01GM095550 from the National Institute of General Medical Sciences to Y.T., and also in part by P30ES025128 from the National Institute of Environmental Health Sciences to the Center for Human Health and the Environment (CHHE). A.R.B. was supported by NIH Training Grant T32ES007046 from the National Institute of Environmental Health Sciences.

AUTHOR CONTRIBUTIONS

M.M. and Y.T. designed the study, performed experiments, analyzed data, and wrote the manuscript. M.M. also prepared the figures and tables and performed the statistical analyses. A.R.B. designed the study and performed the experiments. All authors approved the manuscript.

DECLARATION OF INTERESTS

The authors declare no competing interests.

Received: September 19, 2017
Revised: June 29, 2018
Accepted: October 5, 2018
Published: November 15, 2018

REFERENCES

Anderson, C.P., Shen, M., Eisenstein, R.S., and Leibold, E.A. (2012). Mammalian iron metabolism and its control by iron regulatory proteins. Biochim. Biophys. Acta *1823*, 1468–1483.

Bogdan, A.R., Miyazawa, M., Hashimoto, K., and Tsuji, Y. (2016). Regulators of iron homeostasis: new players in metabolism, cell death, and disease. Trends Biochem. Sci. *41*, 274–286.

Calandrini, V., Nguyen, T.H., Arnesano, F., Galliani, A., Ippoliti, E., Carloni, P., and Natile, G. (2014). Structural biology of cisplatin complexes with cellular targets: the adduct with human copper chaperone atox1 in aqueous solution. Chemistry *20*, 11719–11725.

Chan, K.T., Choi, M.Y., Lai, K.K., Tan, W., Tung, L.N., Lam, H.Y., Tong, D.K., Lee, N.P., and Law, S. (2014). Overexpression of transferrin receptor CD71 and its tumorigenic properties in esophageal squamous cell carcinoma. Oncol. Rep. *31*, 1296–1304.

Ciriello, G., Gatza, M.L., Beck, A.H., Wilkerson, M.D., Rhie, S.K., Pastore, A., Zhang, H., McLellan, M., Yau, C., Kandoth, C., et al. (2015). Comprehensive molecular portraits of invasive lobular breast cancer. Cell *163*, 506–519.

Dasari, S., and Tchounwou, P.B. (2014). Cisplatin in cancer therapy: molecular mechanisms of action. Eur. J. Pharmacol. *740*, 364–378.

DeRusso, P.A., Philpott, C.C., Iwai, K., Mostowski, H.S., Klausner, R.D., and Rouault, T.A. (1995). Expression of a constitutive mutant of iron regulatory protein 1 abolishes iron homeostasis in mammalian cells. J. Biol. Chem. *270*, 15451–15454.

Dixon, S.J., and Stockwell, B.R. (2014). The role of iron and reactive oxygen species in cell death. Nat. Chem. Biol. *10*, 9–17.

Drakesmith, H., Nemeth, E., and Ganz, T. (2015). Ironing out ferroportin. Cell Metab. *22*, 777–787.

Galy, B., Ferring-Appel, D., Kaden, S., Grone, H.J., and Hentze, M.W. (2008). Iron regulatory proteins are essential for intestinal function and control key iron absorption molecules in the duodenum. Cell Metab. *7*, 79–85.

Goossen, B., Caughman, S.W., Harford, J.B., Klausner, R.D., and Hentze, M.W. (1990). Translational repression by a complex between the iron-responsive element of ferritin mRNA and its specific cytoplasmic binding protein is position-dependent in vivo. EMBO J. *9*, 4127–4133.

Gregg, R.W., Molepo, J.M., Monpetit, V.J., Mikael, N.Z., Redmond, D., Gadia, M., and Stewart, D.J. (1992). Cisplatin neurotoxicity: the relationship between dosage, time, and platinum concentration in neurologic tissues, and morphologic evidence of toxicity. J. Clin. Oncol. *10*, 795–803.

Habashy, H.O., Powe, D.G., Staka, C.M., Rakha, E.A., Ball, G., Green, A.R., Aleskandarany, M., Paish, E.C., Douglas Macmillan, R., Nicholson, R.I., et al. (2010). Transferrin receptor (CD71) is a marker of poor prognosis in breast cancer and can predict response to tamoxifen. Breast Cancer Res. Treat. *119*, 283–293.

Henderson, B.R., Menotti, E., and Kuhn, L.C. (1996). Iron regulatory proteins 1 and 2 bind distinct sets of RNA target sequences. J. Biol. Chem. *271*, 4900–4908.

Hentze, M.W., Muckenthaler, M.U., Galy, B., and Camaschella, C. (2010). Two to tango: regulation of mammalian iron metabolism. Cell *142*, 24–38.

Iwasaki, K., Mackenzie, E.L., Hailemariam, K., Sakamoto, K., and Tsuji, Y. (2006). Hemin-mediated regulation of an antioxidant-responsive element of the human ferritin H gene and role of Ref-1 during erythroid differentiation of K562 cells. Mol. Cell. Biol. *26*, 2845–2856.

Jeong, S.Y., Crooks, D.R., Wilson-Ollivierre, H., Ghosh, M.C., Sougrat, R., Lee, J., Cooperman, S., Mitchell, J.B., Beaumont, C., and Rouault, T.A. (2011). Iron insufficiency compromises motor neurons and their mitochondrial function in Irp2-null mice. PLoS One *6*, e25404.

Karasawa, T., Sibrian-Vazquez, M., Strongin, R.M., and Steyger, P.S. (2013). Identification of cisplatin-binding proteins using agarose conjugates of platinum compounds. PloS One *8*, e66220.

Kelland, L. (2007). The resurgence of platinum-based cancer chemotherapy. Nat. Rev. Cancer *7*, 573–584.

Kerins, M.J., Vashisht, A.A., Liang, B.X., Duckworth, S.J., Praslicka, B.J., Wohlschlegel, J.A., and Ooi, A. (2017). Fumarate mediates a chronic proliferative signal in fumarate hydratase-inactivated cancer cells by increasing transcription and translation of ferritin genes. Mol. Cell. Biol. *37*, https://doi.org/10.1128/MCB.00079-17.

Kuhn, L.C. (2015). Iron regulatory proteins and their role in controlling iron metabolism. Metallomics *7*, 232–243.

LaVaute, T., Smith, S., Cooperman, S., Iwai, K., Land, W., Meyron-Holtz, E., Drake, S.K., Miller, G., Abu-Asab, M., Tsokos, M., et al. (2001). Targeted deletion of the gene encoding iron regulatory protein-2 causes misregulation of iron metabolism and neurodegenerative disease in mice. Nat. Genet. *27*, 209–214.

Lui, G.Y., Kovacevic, Z., Richardson, V., Merlot, A.M., Kalinowski, D.S., and Richardson, D.R. (2015). Targeting cancer by binding iron: dissecting cellular signaling pathways. Oncotarget *6*, 18748–18779.

Ma, Y., Abbate, V., and Hider, R.C. (2015). Iron-sensitive fluorescent probes: monitoring intracellular iron pools. Metallomics *7*, 212–222.

MacKenzie, E.L., Iwasaki, K., and Tsuji, Y. (2008). Intracellular iron transport and storage: from molecular mechanisms to health implications. Antioxid. Redox Signal. *10*, 997–1030.

Maffettone, C., Chen, G., Drozdov, I., Ouzounis, C., and Pantopoulos, K. (2010). Tumorigenic properties of iron regulatory protein 2 (IRP2) mediated by its specific 73-amino acids insert. PLoS One *5*, e10163.

Magro, G., Cataldo, I., Amico, P., Torrisi, A., Vecchio, G.M., Parenti, R., Asioli, S., Recupero, D., D'Agata, V., Mucignat, M.T., et al. (2011). Aberrant expression of TfR1/CD71 in thyroid carcinomas identifies a novel potential diagnostic marker and therapeutic target. Thyroid *21*, 267–277.

Meyron-Holtz, E.G., Ghosh, M.C., Iwai, K., LaVaute, T., Brazzolotto, X., Berger, U.V., Land, W., Ollivierre-Wilson, H., Grinberg, A., Love, P., et al. (2004). Genetic ablations of iron regulatory proteins 1 and 2 reveal why iron regulatory protein 2 dominates iron homeostasis. EMBO J. *23*, 386–395.

Miyazawa, M., Bogdan, A.R., Hashimoto, K., and Tsuji, Y. (2018). Regulation of transferrin receptor-1 mRNA by the interplay between IRE-binding proteins and miR-7/miR-141 in the 3'-IRE stem-loops. RNA *24*, 468–479.

Miyazawa, M., and Tsuji, Y. (2014). Evidence for a novel antioxidant function and isoform-specific regulation of the human p66Shc gene. Mol. Biol. Cell *25*, 2116–2127.

Muckenthaler, M., Gray, N.K., and Hentze, M.W. (1998). IRP-1 binding to ferritin mRNA prevents the recruitment of the small ribosomal subunit by the cap-binding complex eIF4F. Mol. Cell *2*, 383–388.

Mullner, E.W., Neupert, B., and Kuhn, L.C. (1989). A specific mRNA binding factor regulates the iron-dependent stability of cytoplasmic transferrin receptor mRNA. Cell *58*, 373–382.

O'Donnell, K.A., Yu, D., Zeller, K.I., Kim, J.W., Racke, F., Thomas-Tikhonenko, A., and Dang, C.V. (2006). Activation of transferrin receptor 1 by c-Myc enhances cellular proliferation and tumorigenesis. Mol. Cell. Biol. *26*, 2373–2386.

Prutki, M., Poljak-Blazi, M., Jakopovic, M., Tomas, D., Stipancic, I., and Zarkovic, N. (2006). Altered iron metabolism, transferrin receptor 1 and ferritin in patients with colon cancer. Cancer Lett. *238*, 188–196.

Ray, P.D., Huang, B.W., and Tsuji, Y. (2012). Reactive oxygen species (ROS) homeostasis and redox regulation in cellular signaling. Cell Signal. *24*, 981–990.

Salahudeen, A.A., Thompson, J.W., Ruiz, J.C., Ma, H.W., Kinch, L.N., Li, Q., Grishin, N.V., and Bruick, R.K. (2009). An E3 ligase possessing an iron-responsive hemerythrin domain is a regulator of iron homeostasis. Science *326*, 722–726.

Saletta, F., Suryo Rahmanto, Y., Siafakas, A.R., and Richardson, D.R. (2011). Cellular iron depletion and the mechanisms involved in the iron-dependent regulation of the growth arrest and DNA damage family of genes. J. Biol. Chem. *286*, 35396–35406.

Schalinske, K.L., Blemings, K.P., Steffen, D.W., Chen, O.S., and Eisenstein, R.S. (1997). Iron regulatory protein 1 is not required for the modulation of ferritin and transferrin receptor expression by iron in a murine pro-B lymphocyte cell line. Proc. Natl. Acad. Sci. U S A *94*, 10681–10686.

Selby, J.V., and Friedman, G.D. (1988). Epidemiologic evidence of an association between body iron stores and risk of cancer. Int. J. Cancer *41*, 677–682.

Smith, S.R., Ghosh, M.C., Ollivierre-Wilson, H., Hang Tong, W., and Rouault, T.A. (2006). Complete loss of iron regulatory proteins 1 and 2 prevents viability of murine zygotes beyond the blastocyst stage of embryonic development. Blood Cells Mol. Dis. *36*, 283–287.

Stevens, R.G., Jones, D.Y., Micozzi, M.S., and Taylor, P.R. (1988). Body iron stores and the risk of cancer. N. Engl. J. Med. *319*, 1047–1052.

Thompson, H.J., Kennedy, K., Witt, M., and Juzefyk, J. (1991). Effect of dietary iron deficiency or excess on the induction of mammary carcinogenesis by 1-methyl-1-nitrosourea. Carcinogenesis *12*, 111–114.

Torti, S.V., and Torti, F.M. (2013). Iron and cancer: more ore to be mined. Nat. Rev. Cancer *13*, 342–355.

Toyokuni, S. (2014). Iron and thiols as two major players in carcinogenesis: friends or foes? Front. Pharmacol. *5*, 200.

Tsuji, Y. (2005). JunD activates transcription of the human ferritin H gene through an antioxidant response element during oxidative stress. Oncogene *24*, 7567–7578.

Vashisht, A.A., Zumbrennen, K.B., Huang, X., Powers, D.N., Durazo, A., Sun, D., Bhaskaran, N., Persson, A., Uhlen, M., Sangfelt, O., et al. (2009). Control of iron homeostasis by an iron-regulated ubiquitin ligase. Science *326*, 718–721.

Wang, J., and Pantopoulos, K. (2002). Conditional derepression of ferritin synthesis in cells expressing a constitutive IRP1 mutant. Mol. Cell. Biol. *22*, 4638–4651.

Wang, J., and Pantopoulos, K. (2011). Regulation of cellular iron metabolism. Biochem. J. *434*, 365–381.

Wang, W., Deng, Z., Hatcher, H., Miller, L.D., Di, X., Tesfay, L., Sui, G., D'Agostino, R.B., Jr., Torti, F.M., and Torti, S.V. (2014). IRP2 regulates breast tumor growth. Cancer Res. *74*, 497–507.

Wilkinson, N., and Pantopoulos, K. (2013). IRP1 regulates erythropoiesis and systemic iron homeostasis by controlling HIF2alpha mRNA translation. Blood *122*, 1658–1668.

Will, J., Wolters, D.A., and Sheldrick, W.S. (2008). Characterisation of cisplatin binding sites in human serum proteins using hyphenated multidimensional liquid chromatography and ESI tandem mass spectrometry. ChemMedChem *3*, 1696–1707.

Wilson, B.R., Bogdan, A.R., Miyazawa, M., Hashimoto, K., and Tsuji, Y. (2016). Siderophores in iron metabolism: from mechanism to therapy potential. Trends Mol. Med. *22*, 1077–1090.

Yu, Y., and Richardson, D.R. (2011). Cellular iron depletion stimulates the JNK and p38 MAPK signaling transduction pathways, dissociation of ASK1-thioredoxin, and activation of ASK1. J. Biol. Chem. *286*, 15413–15427.

Zumbrennen, K.B., Wallander, M.L., Romney, S.J., and Leibold, E.A. (2009). Cysteine oxidation regulates the RNA-binding activity of iron regulatory protein 2. Mol. Cell. Biol. *29*, 2219–2229.

Zumbrennen-Bullough, K.B., Becker, L., Garrett, L., Holter, S.M., Calzada-Wack, J., Mossbrugger, I., Quintanilla-Fend, L., Racz, I., Rathkolb, B., Klopstock, T., et al. (2014). Abnormal brain iron metabolism in Irp2 deficient mice is associated with mild neurological and behavioral impairments. PLoS One *9*, e98072.

STAR★METHODS

KEY RESOURCES TABLE

REAGENT or RESOURCE	SOURCE	IDENTIFIER
Antibodies		
Rabbit polyclonal anti-ferritin H	Santa Cruz Biotechnology	Cat# sc-25617; RRID: AB_2232020
Mouse monoclonal anti-NQO1	Santa Cruz Biotechnology	Cat# sc-32793; RRID: AB_628036
Goat polyclonal anti-IRP1	Santa Cruz Biotechnology	Cat# sc-14216; RRID: AB_2223767
Mouse monoclonal anti-IRP2	Santa Cruz Biotechnology	Cat# sc-33682; RRID: AB_2126703
Rabbit polyclonal anti-ferroportin 1	Novus	Cat# NBP1-21502; RRID: AB_2302075
Mouse monoclonal anti-GAPDH	Chemicon	Cat# MAB374; RRID: AB_2107445
Rabbit polyclonal anti-ferritin L	Sigma-Aldrich	Cat# F5012; RRID: AB_259622
Rabbit polyclonal anti-β-actin	Sigma-Aldrich	Cat# A2066; RRID: AB_476693
Mouse monoclonal Anti-HA Tag	BioLegend	Cat# 901514; RRID: AB_291552
Mouse normal IgG	Santa Cruz Biotechnology	Cat# sc-2025; RRID: AB_737182
Mouse monoclonal anti-Flag antibody	Sigma	Cat# F3165; RRID: AB_259529
Rabbit polyclonal anti-TfR1	Abcam	Cat# ab84036; RRID: AB_10673794
Biological Samples		
SW480 human colon adenocarcinoma-derived tumor tissue by xenografts in NSG mice	This paper	N/A
Chemicals, Peptides, and Recombinant Proteins		
Dulbecco's modified Eagle medium (DMEM)	Corning	50-003-PC
Fetal bovine serum (FBS)	Mediatech	35-010-CV
Minimum Essential Medium (MEM)	Corning	50-011-PC
Bovine insulin	SIGMA	I-6634
Sodium pyruvate	Corning	MT25000CI
RPMI1640	Corning	50-020-PC
Cisplatin	Calbiochem	232120
Cisplatin	TSZChem	RYG01
Cisplatin	Alexis Biochemicals	ALX-400-040
Carboplatin	Alexis Biochemicals	ALX-400-041
$PtCl_2$ Platinum(II) chloride	Acros Organics	195382500
Ammonium iron(III) citrate (FAC)	Sigma-Aldrich	F5879
Deferoxamine mesylate salt (DFO)	Sigma	D9533
Hydrogen peroxide	Calbiochem	386790
t-butyl hydroperoxide (tBHP)	Sigma-Aldrich	B-2633
Transplatin	Aldrich	P1525
TRI Reagent RT	Molecular Research Center	RT111
iTaq Universal SYBR Green Supermix	Bio-Rad	1725125
Polyethylenimine	Polysciences, Inc	23966
Luciferase cell culture lysis reagent	Promega	E1531
Luciferase assay substrate	Promega	E1501
Streptavidin-agarose beads	Invitrogen	15942
Human Myc-Flag-tagged IRP2 protein	Origene	TP321385
[γ-^{32}P] ATP	PerkinElmer	BLU002A
T4 polynucleotide kinase	New England Biolabs	M0201
Crystal violet	EM Science	CX2096-2
Lipofectamine RNAiMAX	Invitrogen	13778150
Calcein-AM	BioLegend	425201

(*Continued on next page*)

Continued

REAGENT or RESOURCE	SOURCE	IDENTIFIER
protein G magnetic beads	Bio-Rad	1614023
Matrigel® Matrix	Corning	354234
Critical Commercial Assays		
QuikChange II Site-Directed Mutagenesis Kit	Agilent Technologies	200524
iScript cDNA Synthesis Kit	Bio-Rad	1708891
Caspase 3/7 Glo assay kit	Promega	G8090
RNAqueous®-Micro Total RNA Isolation Kit	Ambion	AM1931
Deposited Data		
Breast invasive carcinoma patients (TCGA, *Cell* Ciriello et al., 2015) database in cBioPortal	cBioPortal	http://www.cbioportal.org/
Experimental Models: Cell Lines		
SW480 human colon adenocarcinoma	ATCC	CCL-228
MCF7 human breast adenocarcinoma	ATCC	HTB-22
HeLa human cervix adenocarcinoma	ATCC	CCL-2
HepG2 human hepatocellular carcinoma	ATCC	HB-8065
HEK293 immortalized human embryonic kidney cells	ATCC	CRL-1573
K562 human erythroleukemia	ATCC	CCL-243
Experimental Models: Organisms/Strains		
NOD.Cg-*Prkdc*^{scid} *IL2rg*^{tm1Wjl}/SzJ (NSG) mouse strain	Jackson Laboratory	005557
Oligonucleotides		
Biotin-labeled ferritin H IRE probes (Biotin-5'-GGUUUCCUGCUUCAACAGUGCUUGGACGGAAC-3')	This paper	N/A
IRP1 C437S mutation primer set for QuikChange II Site-Directed Mutagenesis	Zumbrennen et al., 2009	N/A
Primers for QuikChange II Site-Directed Mutagenesis (See Table S3)	This paper	N/A
Primers for real time PCR (See Table S1)	This paper	N/A
siRNA sequences (See Table S2)	This paper	N/A
Recombinant DNA		
pCMV-SPORT6 IRP1 (human) plasmid	Open Biosystems	MHS1010-58195
pCR4-TOPO-IRP2 (human) plasmid	Open Biosystems	MHS4426-99239389
Human ferritin H 5'-UTR with IRE (0.33kb)	This paper	-0.2kb PCR DNA containing the h-Ferritin H IRE was cloned into Tsuji, 2005 (XhoI/HindIII)
Human ferritin H 5'-UTR without IRE (0.15kb)	Tsuji, 2005	N/A
pBluescriptSK(-) plasmid	Stratagene	212206
Firefly luciferase gene (pGL3 basic)	Promega	E1751
pcDNA3 plasmid	Invitrogen	V790-20
pCMVSPORT6SLC40A1	Dharmacon	MHS6278-202801506
Software and Algorithms		
SPSS Statistics 24 software	IBM	N/A
cBioPortal	Center for Molecular Oncology at Memorial Sloan Kettering Cancer Center	http://www.cbioportal.org/

CONTACT FOR REAGENT AND RESOURCE SHARING

Further information and requests for resources and reagents should be directed to and will be fulfilled by the Lead Contact, Yoshiaki Tsuji (ytsuji@ncsu.edu).

EXPERIMENTAL MODEL AND SUBJECT DETAILS

Animal Studies

The protocol of the xenograft study was approved by North Carolina State University Institutional Animal Care and Use Committee (IACUC) (Protocol # 16-089). For this experiment, 3-6 months male NSG mice were used.

METHOD DETAILS

Cell Culture and Chemicals

SW480 human colon adenocarcinoma (established from 50 years old male), MCF7 human breast adenocarcinoma (from 69 years old female), HeLa human cervix adenocarcinoma (from 31 years old female), HepG2 human hepatocellular carcinoma (from 15 years old male), K562 human erythroleukemia (from 53 years old female), HEK293 immortalized human embryonic kidney cells (from fetus female) were obtained from the American Type Culture Collection (ATCC, Manassas, VA). SW480 cells were cultured in Dulbecco's modified Eagle medium (DMEM) (50-003-PC; Corning, Manassas, VA) containing 10% fetal bovine serum (FBS) (35-010-CV; Mediatech, Manassas, VA). MCF7 cells were cultured in Minimum Essential Medium (MEM) (50-011-PC; Corning) containing 10% FBS with 10 μg/mL bovine insulin, and 1 mM sodium pyruvate. HeLa, HepG2, and HEK293 cells were cultured in MEM containing 10% FBS. K562 cells were cultured in RPMI1640 (50-020-PC; Corning) containing 10% FBS. They were cultured in a humidified 95% incubator (37°C, 5% CO_2). Cisplatin (three different cisplatin suppliers, Calbiochem, La Jolla, CA, TSZChem, Framingham, MA, and Alexis Biochemicals, San Diego, CA, all of which showed the same effects), carboplatin (Alexis Biochemicals), $PtCl_2$ (Acros Organics, Geel-Belgium, NJ), ferric ammonium citrate (FAC, Sigma-Aldrich, St. Louis, MO), desferrioxamine (DFO, Sigma, St. Louis, MO), Hydrogen peroxide (H_2O_2) (Calbiochem), and t-butyl hydroperoxide (tBHP) (Sigma-Aldrich) were dissolved in distilled ultrapure water. Transplatin (Aldrich, St. Louis, MO) was dissolved in dimethyl sulfoxide at 10 mg/mL for stock solution.

Western Blot and Antibodies

Western blot analysis was performed as previously described (Miyazawa and Tsuji, 2014) except for no boiling of samples for detection of ferroportin. Antibodies used in this work were anti-ferritin H (sc-25617), anti-NQO1 (sc-32793), anti-IRP1 (sc-14216), anti-IRP2 (sc-33682) from Santa Cruz Biotechnology (Santa Cruz, CA), anti-TfR1 (ab84036) from Abcam (Cambridge, MA); anti-ferroportin 1 (NBP1-21502) from Novus (Littleton, CO); anti-β-actin (A2066) and anti-ferritin L (F5012) from Sigma (St. Louis, MO); anti-GAPDH (MAB374) from Chemicon (Temecula, CA); Anti-HA Tag (HA.11, 901514) from BioLegend (San Diego, CA).

Real Time PCR

Total RNA was isolated with TRI Reagent RT (Molecular Research Center, Cincinnati, OH) and cDNA was synthesized using iScript cDNA Synthesis Kit (Bio-Rad, Hercules, CA) with 500 ng of total RNA as a template. Equal amounts of cDNA were amplified by 30-45 cycles of denaturing for 10 sec at 95°C and annealing and extension for 45 sec at 60°C in a CFX96 Real-Time PCR System with iTaq Universal SYBR Green Supermix (Bio-Rad). Sequences of specific human primer pairs are shown in Table S1.

Luciferase Assay

Human ferritin H 5'-UTR with IRE (0.35kb) luciferase plasmid was constructed by insertion of 0.2kb PCR DNA containing the h-ferritin H IRE into XhoI/HindIII sites of the ferritin H promoter luciferase without IRE (0.15kb (Tsuji, 2005)) in the pBluescriptSK(-) plasmid. The luciferase reporter plasmid containing mutant ferritin H IRE (Henderson et al., 1996) was constructed by QuikChange II Site-Directed Mutagenesis (Agilent Technologies, Santa Clara, CA) according to the manufacturer's protocol. SW480 or HepG2 cells were transfected with these reporter plasmids with Polyethylenimine (linear, ~25kDa, Polysciences, Inc) and treated with cisplatin, transplatin, carboplatin, $PtCl_2$, FAC, or DFO for 18-24 h. Cell lysates in luciferase cell culture lysis reagent (Promega, Madison, WI) were incubated with the luciferase assay substrate (E1501; Promega). Luciferase activates were measured by GloMax 20/20 (Promega).

Pull-Down mRNA-Protein Binding Assay

200 μg whole-cell lysates were incubated with 10 μg biotin-labeled ferritin H IRE probes (Biotin-5'-GGUUUCCUGCUUCAACAGUG CUUGGACGGAAC-3′) and streptavidin-agarose beads (Invitrogen, Carlsbad, CA) in PBS^- containing 0.5% NP40 and inhibitors of protease and RNase (buffer A) at 4°C. Precipitates with beads were washed with buffer A, and subjected to Western blot with anti-HA, anti-IRP1 or anti-IRP2 antibody.

Electrophoresis Mobility Shift Assay (EMSA)

A human ferritin H IRE probe was end-labeled with [γ-^{32}P] ATP and T4 polynucleotide kinase at 37°C for 10 min. Human Myc-Flag-tagged IRP2 protein (50 ng/μL, Origene, Rockville, MD) pre-incubated with cisplatin or carboplatin at room temperature for 16 h were incubated with ^{32}P-labeled ferritin H IRE probe at room temperature for 1 h. Protein-RNA complexes were separated on 4% polyacrylamide-0.5% TBE gel electrophoresis and subjected to autoradiography. Mouse normal IgG (sc-2025; Santa Cruz) and anti-Flag antibody (F3165; Sigma) were used to verify the IRP2-IRE binding complex.